Dynamical Investigation of Crawling Motion System based on a Multistable Tensegrity Structure

Philipp Schorr[1], Valter Böhm[2], Lena Zentner[3] and Klaus Zimmermann[1]
[1]*Technical Mechanics Group, Department of Mechanical Engineering, Technical University of Ilmenau, Max-Planck-Ring 12, 98693 Ilmenau, Germany*
[2]*Technical Mechanics, Department of Mechanical Engineering, Ostbayerische Technische Hochschule Regensburg, Galgenbergstr. 30, 93053 Regensburg, Germany*
[3]*Compliant Systems Group, Department of Mechanical Engineering, Technical University of Ilmenau, Max-Planck-Ring 12, 98693 Ilmenau, Germany*

Keywords: Worm-like Motion, Multistable Tensegrity Structure.

Abstract: The basic idea of this article is the utilization of the multistable character of a compliant tensegrity structure to control the direction of motion of a crawling motion system. A crawling motion system basing on a two-dimensional tensegrity structure with multiple stable equilibrium states is considered. This system is in contact with a horizontal plane due to gravity. For a selected harmonic actuation of the system small oscillations around the given equilibrium state of the tensegrity structure occur and the corresponding uniaxial motion of the system is evaluated. A change of the equilibrium state of the tensegrity structure yields to novel configuration of the entire system. Moreover, the motion behavior of the novel configuration is totally different although the actuation strategy is not varied. In particular, the direction of motion changes. Therefore, this approach enables a uniaxial bidirectional crawling motion with a controllable direction of motion using only one actuator with a selected excitation frequency.

SCITEPRESS SCIENCE AND TECHNOLOGY PUBLICATIONS

1 INTRODUCTION

The increasing significance of mobile robotics in engineering applications requires a continuous improvement of the current systems respective to the operating sensors and actuators. Moreover, as consequence of the advanced demands on those systems even the investigation of novel motion principles is necessary. For example, applications like the minimal invasive surgery allow only an extremely limited working space which prevent the use of conventional motion systems basing on wheels or legs. Therefore, innovative motion principles basing on the direct interaction to the environment are required.

A promising approach is the investigation of crawling motion systems. This principle is copied from the motion behavior of earth worms observed in the nature. The peristaltic motion bases on the alternating shortening and lengthening of several body segments. Moreover, the presence of spike which are added at the body of the earth worm are essential for the motion. Hence, a forward or backward motion occurs depending on the orientation of these spikes.

Beside the biological aspects of the worm-like motion groups of researchers are also interested in this motion principle from the mechanical point of view. In (Steigenberger and Behn, 2012), (Zimmermann et al., 2009a) and (Zimmermann et al., 2013) the earth worm is modeled by a finite number of rigid body which are connected by kinematic drives. The mechanical behavior of the mentioned spikes is modeled by anisotropic friction properties and the occurring motion behavior is investigated. But as consequence of the anisotropy of the friction properties a preferred direction of motion occurs and the use of the opposite direction of motion is not possible for a harmonic actuation. In (Bolotnik et al., 2006) and (Zimmermann et al., 2009b) the actuation of an additional internal mass is investigated in order to control the direction of motion for isotropic friction properties. Moreover, in (Fang and Xu, 2011) and (Fang and Xu, 2012) the actuation by the kinematic drive is varied to maximize the steady state velocity. However, for isotropic friction properties advanced requirements are demanded on the actuator of the system. Hence, the current state of the art not satisfying.

The use of compliant tensegrity structures in mobile robotics enables advantages like high weight-to-

Schorr, P., Böhm, V., Zentner, L. and Zimmermann, K.
Dynamical Investigation of Crawling Motion System based on a Multistable Tensegrity Structure.
DOI: 10.5220/0006852701220130
In *Proceedings of the 15th International Conference on Informatics in Control, Automation and Robotics (ICINCO 2018) - Volume 2*, pages 122-130
ISBN: 978-989-758-321-6
Copyright © 2018 by SCITEPRESS – Science and Technology Publications, Lda. All rights reserved

load ratio, shock resistance and adjustable dynamical behavior. Therefore, those structures are considered for the application in motion systems. In (Sabelhaus et al., 2015), (Kim et al., 2016), (Hustig-Schultz et al., 2016), (Liu et al., 2016) and (Chen et al., 2017) the capability of shape change is used to realize successive tilting sequences which yield to a controllable motion. The shape change is realized by the manipulation of mechanical parameter values. Furthermore, the use of tensegrity structures in vibration driven motion systems is investigated in (Rieffel et al., 2010), (Böhm and Zimmermann, 2013), (Böhm et al., 2013), (Khazanov et al., 2014) and (Böhm et al., 2015). The dynamics of the tensegrity structure can be influenced by varying the prestress states. This is also realized by a variation of the mechanical properties. In (Schorr et al., 2017) a vibration driven motion system based on a multistable tensegrity structure is investigated. The dynamical properties are varied to discrete values by changing the equilibrium state. In (Tietz et al., 2013) a crawling motion system is realized by a tensegrity structure consisting of several segments connected in series. The actuation strategy is investigated for different evironmental conditions. However, because of number of segments many actuators are required and a enormous control effort is necessary.

In this article a crawling motion system basing on a two-dimensional multistable tensegrity structure inspired by (Böhm et al., 2017) and (Sumi et al., 2017) is considered. The system is in contact to a horizontal plane due to gravity. A selected harmonic actuation of the system yields to a crawling motion. As consequence of a change of the equilibrium state the configuration of the entire systems is modified (contact points are changing as consequence of a tilting sequence). Therefore, totally different motion characteristics occur for an identical actuation strategy. In particular, the direction of motion can be controlled by changing the equilibrium state of the tensegrity structure. This idea is illustrated in Figure 1.

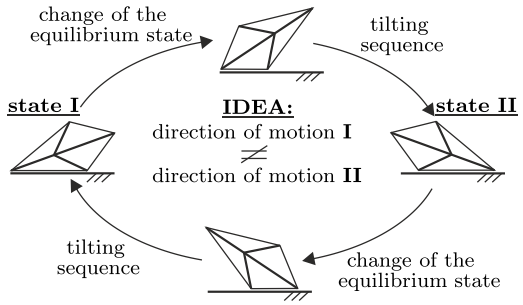

Figure 1: Supposed behavior of the motion system.

Thus, this approach enables a uniaxial bidirectional crawling motion with only one actuator using a selected actuation frequency. Therefore, the presence of anisotropic friction properties and the application of high-end actuators is not necessary anymore.

2 MECHANICAL MODEL OF THE MOTION SYSTEM

2.1 Dynamics of the Multistable Tensegrity Structure

The tensegrity structure shown in Figure 2 is considered. This structure consists of 9 members ($j = 1,2,\ldots,9$) which are connected in 5 nodes ($i = 1,2,\ldots,5$). These nodes are modeled as frictionless revolute joints. With regard to the occurring stress at the equilibrium state the members are divided in compressed members and tensioned members. For the given structural topology, the elements $j = 1,2,3$ are classified as compressed members. The members $j = 4,5,6,7,8,9$ are declared as tensioned members.

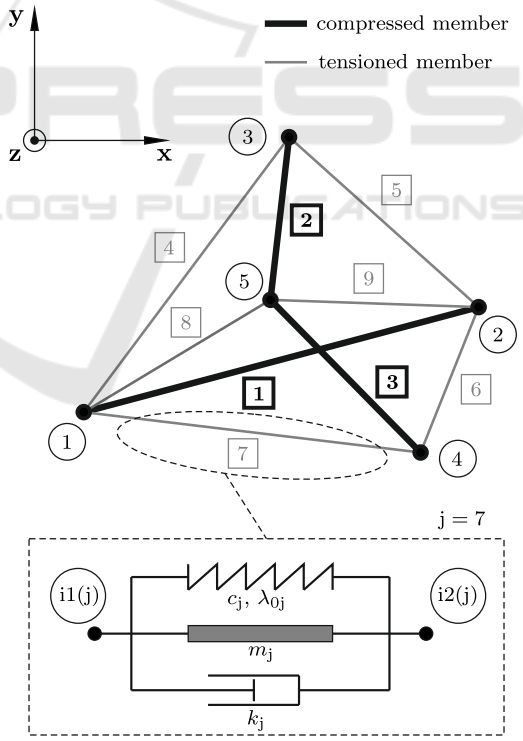

Figure 2: Two-dimensional multistable tensegrity structure and the mechanical model of a single member.

The current configuration of the tensegrity structure is defined by the position of the nodes i. These position are evaluated respective to the Cartesian inertial coordinate system $\{x,y,z\}$ to $\vec{r}_i = (x_i, y_i, z_i)^T$.

Furthermore, the structure is supposed to be two-dimensional in the x-y-plane. Therefore, the z-component of the node positions is identical to zero ($z_i \equiv 0$). This yields to a degree of freedom of 10 for the considered tensegrity structure. As generalized coordinates the components of the node positions x_i and y_i are selected. These parameters are combined in the vector $\vec{q} = (x_1, y_1, x_2, y_2, \ldots, x_5, y_5)^T$.

In order to describe the dynamics of the tensegrity structure all acting loads have to be specified. Therefore, the forces as consequence of the deformations of the members have to be taken into account. The deformation behavior of a single member is modeled with a linear spring which is described by the according stiffness c_j and its initial length $\lambda_{0,j}$. The corresponding energy dissipation as consequence of the material damping properties is given by a linear damper with the damping coefficient k_j. Furthermore, the inertia of each element has to be taken into account. The element j with the mass m_j is modeled by a linear link element known from the finite element method. Therefore, the inertia is given by the according mass matrix. For the following investigations the mass of the tensioned members is assumed to be neglectable ($m_j = 0$ for $j = 4,5,6,7,9$.) The resulting mechanical model of a single member of the tensegrity structure is given by a parallel arrangement of the mentioned components (see Figure 2). The deformation of the member j is given by the position of the node $i1(j)$ at its beginning and the node $i2(j)$ at its end. The corresponding spring force $\vec{F}_{c,j}$ and the damping force $\vec{F}_{k,j}$ are formulated in (1) and (2).

$$\vec{F}_{c,j} = -c_j(|\vec{\lambda}_j| - \lambda_{0,j})\frac{\vec{\lambda}_j}{|\vec{\lambda}_j|}, \quad \vec{\lambda}_j = \vec{r}_{i2(j)} - \vec{r}_{i1(j)} \tag{1}$$

$$\vec{F}_{k,j} = -k_j \frac{\dot{\vec{\lambda}}_j \cdot \vec{\lambda}_j}{|\vec{\lambda}_j|}\frac{\vec{\lambda}_j}{|\vec{\lambda}_j|}, \quad \dot{\vec{\lambda}}_j = \dot{\vec{r}}_{i2(j)} - \dot{\vec{r}}_{i1(j)} \tag{2}$$

With regard to the topology of the tensegrity structure these forces are combined to the vectors $\vec{C}(\vec{q})$ and $\vec{K}(\dot{\vec{q}}, \vec{q})$. This approach is shown in (3) and (4).

$$\vec{C}(\vec{q}) = -\begin{pmatrix} -\vec{F}_{c,1} - \vec{F}_{c,4} - \vec{F}_{c,7} - \vec{F}_{c,8} \\ \vec{F}_{c,1} - \vec{F}_{c,5} - \vec{F}_{c,6} - \vec{F}_{c,9} \\ -\vec{F}_{c,2} + \vec{F}_{c,4} + \vec{F}_{c,5} \\ -\vec{F}_{c,3} + \vec{F}_{c,6} + \vec{F}_{c,7} \\ \vec{F}_{c,2} + \vec{F}_{c,3} + \vec{F}_{c,8} + \vec{F}_{c,9} \end{pmatrix} \tag{3}$$

$$\vec{K}(\dot{\vec{q}}, \vec{q}) = -\begin{pmatrix} -\vec{F}_{k,1} - \vec{F}_{k,4} - \vec{F}_{k,7} - \vec{F}_{k,8} \\ \vec{F}_{k,1} - \vec{F}_{k,5} - \vec{F}_{k,6} - \vec{F}_{k,9} \\ -\vec{F}_{k,2} + \vec{F}_{k,4} + \vec{F}_{k,5} \\ -\vec{F}_{k,3} + \vec{F}_{k,6} + \vec{F}_{k,7} \\ \vec{F}_{k,2} + \vec{F}_{k,3} + \vec{F}_{k,8} + \vec{F}_{k,9} \end{pmatrix} \tag{4}$$

The inertia of the tensegrity structure is taken into account by the mass matrix $\mathbf{M}$. Hence, the nonlinear system of equations of motion shown in (5) results.

$$\mathbf{M}\ddot{q} + \vec{K}(\dot{\vec{q}}, \vec{q}) + \vec{C}(\vec{q}) = \vec{0} \tag{5}$$

For the following investigations the parameter values listed in Table 1 are used.

Table 1: Topology and selected parameter values of the tensegrity structure.

El. j	Nodes i1 − i2	$\lambda_{0,j}$ [m]	c_j [N/m]	k_j [Ns/m]	m_j [kg]
1	1 − 2	0.10	10^6	0.2	0.1
2	3 − 5	0.02	10^6	0.2	0.02
3	4 − 5	0.02	10^6	0.2	0.02
4	1 − 3	0.02	3000	0.2	0
5	2 − 3	0.02	3000	0.2	0
6	2 − 4	0.02	3000	0.2	0
7	1 − 4	0.02	3000	0.2	0
8	1 − 5	0.01	10000	0.2	0
9	2 − 5	0.01	10000	0.2	0

2.2 Modeling of the Crawling Motion System

In order to realize a crawling motion an actuation of the tensegrity structure is required. For the following investigations free length of the tensioned member 8 is manipulated by a harmonic excitation function $s(t) = a\sin(2\pi ft)$ (a - amplitude of excitation, f - actuation frequency). The corresponding actuation force is given in (6).

$$\vec{F}_A(t) = (c_8 s(t) + k_8 \dot{s}(t))\frac{\vec{\lambda}_8}{|\vec{\lambda}_8|} \tag{6}$$

The multistable tensegrity structure is in contact with a horizontal plane due to gravity ($\vec{g} = -g\vec{e}_y$). Therefore, beside the actuation force the equations of motion have to be completed by the gravitational forces as well as the contact forces. Moreover, occurring friction effects at the contact points have to be taken into account.

The gravitational forces are divided into components acting on the nodes i. The resulting force vector $\vec{G}$ is defined in (7).

$$\vec{G} = -\frac{g}{2}(0, m_1, 0, m_1, 0, m_2, 0, m_3, 0, m_2 + m_3)^T \tag{7}$$

The contact interface between the nodes i and the ground is represented by isolated points. The deformation of the ground at those contact points is modelled by a parallel arrangement of a linear damper

$k_g = 100$ Ns/m and a linear spring $c_g = 10^5$ N/m. The deformation of the contact node of the tensegrity structure is assumed to be neglectable. The corresponding contact force at the node i is given by the vector $\vec{F}_{\text{contact,i}} = (F_{\text{F,i}}, F_{\text{N,i}})^{\text{T}}$. The component $F_{\text{F,i}}$ describes the occurring friction forces at the contact node i and $F_{\text{N,i}}$ the acting contact force. The definition of the component $F_{\text{N,i}}$ is given in (8).

$$F_{\text{N,i}} = \begin{cases} 0 & \text{if } y_i \geq 0 \\ -c_g y_i & \text{if } y_i < 0 \text{ and } \dot{y}_i \geq 0 \\ -c_g y_i - k_g \dot{y}_i & \text{else} \end{cases} \quad (8)$$

Occurring friction at the contact nodes are modeled by COULOMB'S LAW OF FRICTION. To model stiction effects like stick-slip despite of the numerical accuracy the friction model is expanded by KARNOPP'S METHOD. Therefore, a parameter $\delta = 10^{-4}$ m/s is introduced. The resulting friction model is given in (2.2). The static and the dynamic friction coefficients are given by the parameters μ_0 and μ. The parameter $F_{\text{res,i}}$ describes the sum of all acting forces except the friction force on the node i along the x-axis.

$$F_{\text{F,i}} = \begin{cases} -\mu F_{\text{N,i}} \operatorname{sign}(\dot{x}_i) & \text{if } |\dot{x}_i| \geq \delta \\ -\mu F_{\text{N,i}} \operatorname{sign}(F_{\text{res,i}}) & \text{if } |\dot{x}_i| < \delta \\ & \text{and } |F_{\text{res,i}}| \geq \mu_0 F_{\text{N,i}} \\ -F_{\text{res,i}} & \text{else} \end{cases} \quad (9)$$

All the mentioned components are combined to the generalized force vector $\vec{Q}(\dot{\vec{q}}, \vec{q}, t)$. Thus, the nonlinear system of equation of motion of the entire crawling motion system formulated in (10) results.

$$\mathbf{M}\ddot{q} + \vec{K}(\dot{\vec{q}}, \vec{q}) + \vec{C}(\vec{q}) = \vec{Q}(\dot{\vec{q}}, \vec{q}, t) \quad (10)$$

$$\text{with } \vec{Q}(\dot{\vec{q}}, \vec{q}, t) = \vec{G} + \begin{pmatrix} \vec{F}_{\text{contact,1}} \\ \vec{F}_{\text{contact,2}} \\ \vec{F}_{\text{contact,3}} \\ \vec{F}_{\text{contact,4}} \\ \vec{F}_{\text{contact,5}} \end{pmatrix} + \begin{pmatrix} -\vec{F}_{\text{A}} \\ \vec{0} \\ \vec{0} \\ \vec{0} \\ \vec{F}_{\text{A}} \end{pmatrix}$$

The resulting mechanical model of the investigated crawling motion system is illustrated in Figure 3.

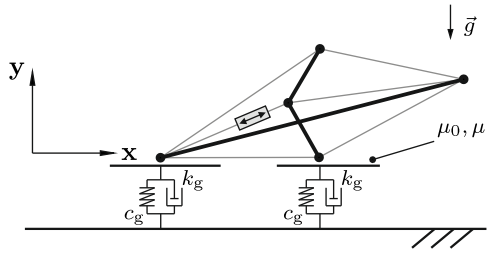

Figure 3: Mechanical model of the crawling motion system - actuation of tensioned member 8 (two-head arrow), nodes 1 and 4 in contact with ground.

3 SIMULATION OF THE CRAWLING MOTION

3.1 Initial Conditions of the Crawling Motion System

The working principle of the crawling motion system requires two equilibrium states **I** and **II** as shown in Figure 1. These configurations have to differ respective to the corresponding contact nodes. For the determination of the equilibrium states the non-actuated motion system ($\vec{F}_{\text{A}} \equiv \vec{0}$) is considered for $\vec{q} = \vec{q}_{\text{eq}}$ and $\dot{\vec{q}} = \vec{0}$. Basing on (10) these conditions yield to a nonlinear system of equations formulated in (11).

$$\vec{C}(\vec{q}_{\text{eq}}) = \vec{Q}(\vec{0}, \vec{q}_{\text{eq}}) \quad (11)$$

However, because of the piecewise smooth contact and friction modelling conventional methods (e.g. NEWTON-RAPHSON) cannot be applied to calculate the configuration $\vec{q}_{\text{eq}}$ and additional numerical effort is required instead. Therefore, at first the interaction between the contact nodes and the ground is approximated by a static support.

Inspired by Figure 1, the nodes 1 and 4 are assumed to be in contact with the ground. The contact is simplified by the supports **A** and **B** (see. Figure 4). The according support reaction are defined by $\vec{A} = (A_x, A_y)^{\text{T}}$ and $\vec{B} = (0, B_y)^{\text{T}}$. This approximation yields to smooth nonlinear system of equations given in (12) which can be solved numerically.

$$\vec{C}(\vec{q}_{\text{eq}}) = \vec{G} + (\vec{A}, \vec{0}, \vec{0}, \vec{B}, \vec{0})^{\text{T}} \quad (12)$$

Each solution of (12) has to be checked additionally ($y_2 \geq 0$, $y_3 \geq 0$, $y_5 \geq 0$). Furthermore, only stable equilibrium configurations are relevant for the following investigation. Therefore, the Hessian of the potential energy is considered. The potential energy is given in (13).

$$E = \sum_{j=1}^{9} \frac{c_j}{2} (|\vec{\lambda}_j| - \lambda_{0,j})^2 + m_j g \frac{\vec{r}_{i1(j)} + \vec{r}_{i2(j)}}{2} \cdot \begin{pmatrix} 0 \\ 1 \end{pmatrix} \quad (13)$$

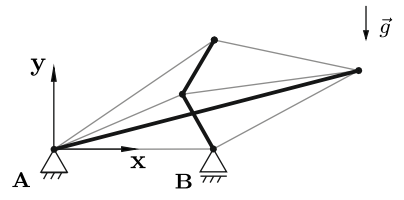

Figure 4: Mechanical model of the crawling motion system for the determination of the relevant stable equilibrium states I and II.

The Hessian of the energy term is evaluated respective to the generalized coordinates $\vec{q}$. An equilibrium state is defined as stable if all eigenvalues of the Hessian are positive. Otherwise, the state is declared as instable and is not taken into account anymore.

This approach yields to two stable configurations of the multistable tensegrity structure (see Figure 5a)). However, finally the support reactions have to be checked. The y-components of those reactions have to be positive. Otherwise, the contact between the node and the ground get lost and a tilting sequence is initiated. Therefore, and in order to take the given contact stiffness into account, a dynamical relaxation of both equilibrium configurations of the system using (10) with $a = 0$ and $\mu_0 = \mu = 0$ is evaluated. The final state $\vec{q}$ after the compliance of the break-off-criteria ($|\dot{\vec{q}}| < 10^{-8}$ m/s and $|\ddot{\vec{q}}| < 10^{-8}$ m/s^2) is declared as $\vec{q}_{\text{eq}}$. Indeed, beside the resulting stable equilibrium state **I** as consequence of a tilting sequence the stable equilibrium state **II** (contact nodes 2 and 4) occurs. This issue confirmes the idea that changing the equilibrium state of the tensegrity structure initiates a tilting sequence of the entire motion system. The resulting equilibrium configurations **I** and **II** of the motion system are illustrated in Figure 5b).

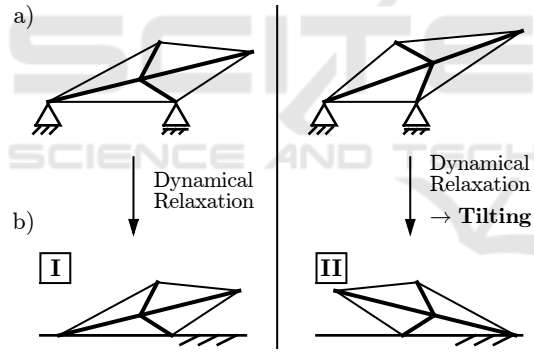

Figure 5: Stable equilibrium states of multistable tensegrity structure - a) as result of the mechanical model shown in Figure 4, b) as result of dynamical relaxation.

This approach was repeated starting from (12) for other combinations of contact nodes (2 and 4, 1 and 3, 2 and 3). Because of the symmetric topology of the structure and the selected parameter values equivalent results occur. As consequence of the approximation by static supports two valid stable equilibrium states are determined. Evaluating a dynamical relaxation one of these states yields to a tilting sequence and the occuring final states $\vec{q}_{\text{eq}}$ are equivalent to the states **I** and **II** shown in Figure 5b). Without loss of generality, for the following investigations the state **I** corresponds to the contact nodes 1 and 4 (state **II** corresponds to the contact nodes 2 and 4).

3.2 Simulation of the Motion Behavior

The nonlinear system of equations of motion of the entire motion system is solved numerically using a RUNGE-KUTTA-METHOD 4$^{\text{th}}$ ORDER with an appropriate step size ($\Delta t = 10^{-4}$ s). As initial condition the configuration **I** or **II** is assumed an the entire system is supposed to be at rest ($\dot{\vec{q}}(t = 0) = \vec{0}$). The motion of the system is simulated for 1100 actuation periods. However, only the steady state solution which is assumed after 1000 actuation periods is evaluated. As amplitude the value $a = 10^{-4}$ m is chosen. Moreover, the motion is evaluated for different friction properties. The motion of the system is illustrated exemplarily on Figure 6 to present the qualitative motion behavior. Moreover, for the considered actuation frequency and friction properties the different initial conditions yield to opposite directions of motion.

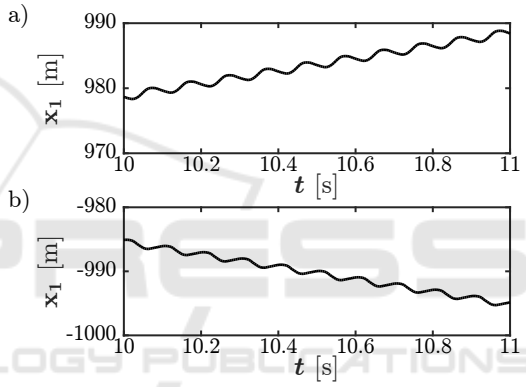

Figure 6: Motion behavior for $f = 10$ Hz, $\mu_0 = \mu = 0.1$ and - a) state **I** as initial condition, b) state **II** as initial condition.

However, as consequence of the transient dynamics a change into another equilibrium state **III** occurs for several actuation frequencies. For this state a collision between the compressed member 2 and 3 appears. Moreover, a reverse change into the state **I** or **II** seems to be difficult because of the low potential energy at this critical state. Therefore, this configuration should be avoided. This configuration is shown in Figure 7 with the nodes 1 and 5 as contact points. Because of the symmetry the same configuration will occur with the contact nodes 2 and 5.

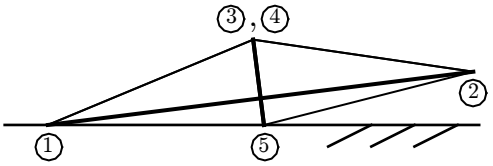

Figure 7: Critical equilibrium state III of the crawling motion system with nodes 1 and 5 as contact nodes.

As indicator of the motion behavior the steady state velocity v of the system is evaluated. This parameter can be calculated considering the velocity of the node i (i $= 1,2,3,4,5$) for an actuation period during the steady state motion. This formula is given in (14). The parameter t_0 is an arbitrary time instance.

$$\mathrm{v} = f \int_{t_0}^{t_0+1/f} \dot{\mathrm{x}}_\mathrm{i}(t)\,\mathrm{d}t \tag{14}$$

The results of the steady state velocity for the equilibrium states **I** and **II** as initial condition with different friction properties are illustrated in Figure 8. The grey areas represent the frequency ranges which lead to a change into the critical equilibrium state **III** as consequence of the transient dynamics.

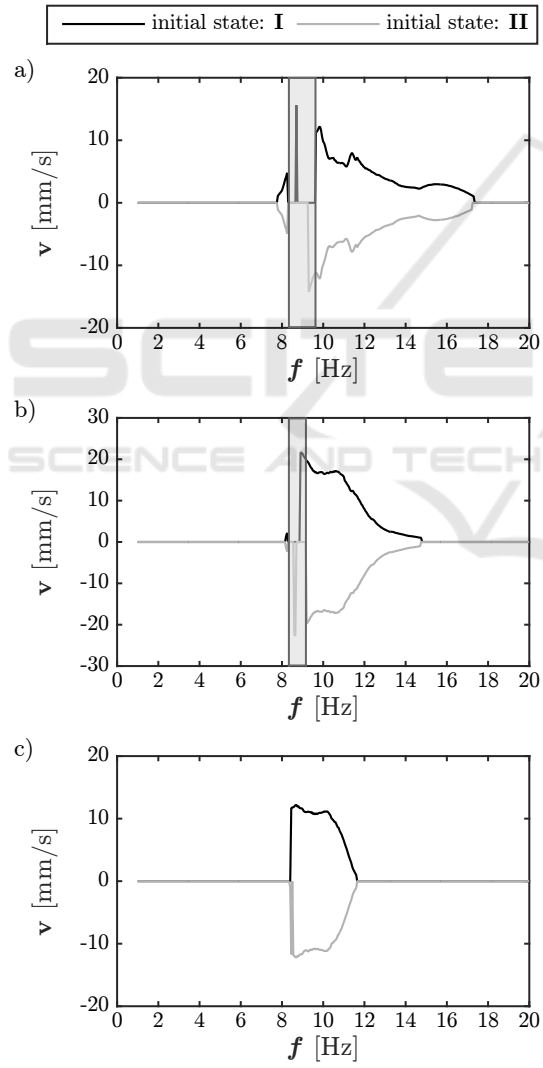

Figure 8: Steady state velocity of the crawling motion system with the different equilibrium configurations as initial conditions and - a) $\mu_0 = \mu = 0.1$, b) $\mu_0 = \mu = 0.2$, c) $\mu_0 = \mu = 0.5$.

These results show that for low actuation frequencies ($f < 8$ Hz) the motion can be considered as inefficient (v < 1 mm/s). For the following frequency range (8 Hz $< f <$ 9.8 Hz) the critical configuration occurs as result of the transient dynamics. However, for actuation frequencies above 10 Hz the results confirm the basic idea of this approach. A motion of the entire system appears as consequence of small oscillations around the stable state **I** or **II**. Indeed, the direction of motion can be varied by changing the equilibrium configuration at the initial state. For the investigated parameters the use of state **I** as initial condition yields to a positive motion (v > 0 mm/s). Assuming the state **II** as initial condition a negative motion (v < 0 mm/s) occurs. Therefore, the results confirm that the multistability of the tensegrity structure can be utilized to control the direction of motion of a crawling motion system.

The influence of the chosen equilibrium state on the direction of motion becomes obvious regarding the corresponding vibration mode of the crawling motion system. In Figure 9 the scaled trajectories of the nodes are exemplarily illustrated. Focusing on the acting contact points, a partial lifting of node 4 can be recognized whereas node 1 is permanent in contact with the horizontal ground. This issue as well as the different contact forces yield to occurrence of friction effects which are essential for the motion. Changing the equilibrium state, a similar effect results. However, the arrangement of the contact nodes is different which affects the direction of motion.

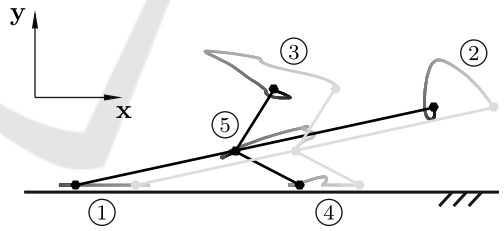

Figure 9: Scaled trajectories of nodes during one actuation period (dark $\rightarrow$ bright) for state I as initial state, $f = 10$ Hz and $\mu_0 = \mu = 0.2$ - scale: $|\mathrm{x}|^* = 10|\mathrm{x}|$, $|\mathrm{y}|^* = 2|\mathrm{y}|$.

3.3 Change of the Equilibrium State

The previous results show that a uniaxial bidirectional motion of the considered system is possible using only one actuator. However, the change between the equilibrium state **I** and **II** has not be considered yet. Of course, different methods and strategies of actuations are possible to realize the mentioned switch between these states. But the following investigation only show that it this change of equilibrium states is possible for a chosen parameter set. Therefore, as actuation strategy of the tensioned member 8 a half-

wave of a sine is selected. The resulting excitation function $u(t)$ is given in (15).

$$u(t) = \begin{cases} a\sin(2\pi f t) & \text{if } t \bmod 1/f \leq \pi \\ 0 & \text{else} \end{cases} \quad (15)$$

The resulting actuation force can be calculated by (6) using $u(t)$ instead of $s(t)$. For the change from state **I** into state **II** the frequency is varied from 10 Hz to 15 Hz and the amplitude from 10^{-4} m to 10^{-3} m. For the reverse change of states, the same frequency range is considered. However the excitation amplitude is supposed to be in a range from -10^{-3} m to -10^{-4} m. The according results are shown in Figure 10.

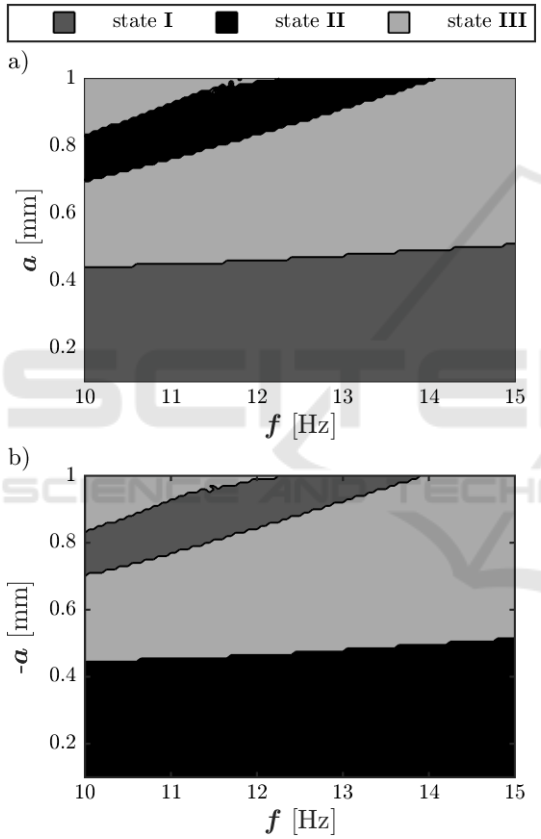

Figure 10: Dynamical investigation of the change of the equilibrium state for a chosen actuation strategy with $\mu_0 = \mu = 0.1$ and - a) state I as initial state, b) state II as initial state.

These results confirm that a change of the equilibrium states is possible for the selected actuation strategy. Therefore, for example the use of only one actuator with an actuation frequency of 10 Hz enables a uniaxial forward and backward motion as well as a change of the equilibrium state (**I** $\rightarrow$ **II** and **II** $\rightarrow$ **I**) utilizing the emphasized multistability of the tensegrity structure.

However, these results show that for a significant parameter range a change into the critical equilibrium state **III** occurs. As mentioned in the previous section a reverse change into another equilibrium state seems to be difficult. Hence, the occurrence of the critical state prevents a further use of the motion system. Therefore, for the construction of a prototype safeguards which prohibit a change into the critical equilibrium state **III** should be taken into account (e.g. mechancial stops).

In order to illustrate the dynamics during the change of the equilibrium states corresponding configurations at different time instances are displayed exemplarily in Figure 11. This figure shows that as consequence of the change of the equilibrium state of the tensegrity structure a tilting sequence of the entire locomotion system occurs as supposed in Figure 1.

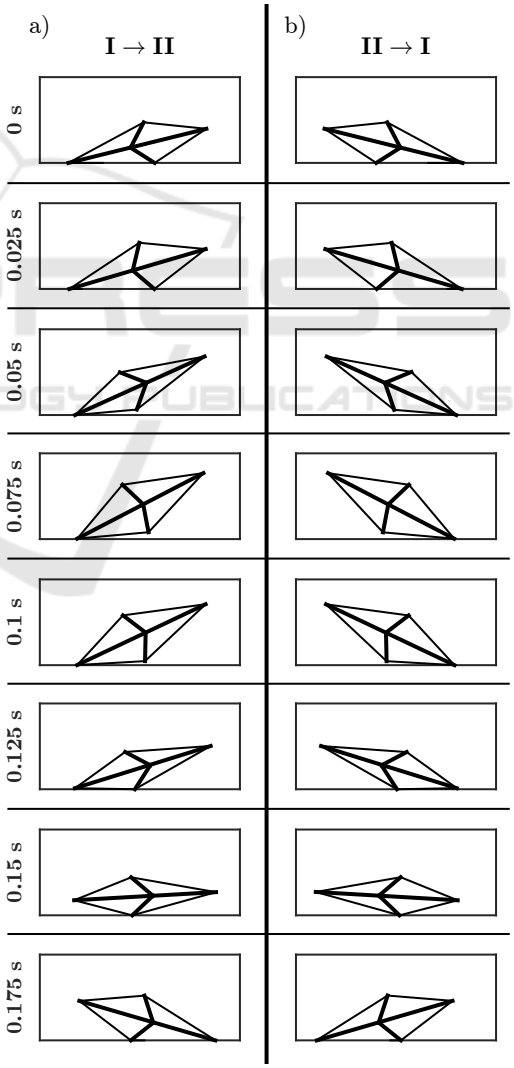

Figure 11: States during the change of the configurations for $\mu_0 = \mu = 0.1$ and $f = 10$ Hz $a = 0.8$ mm, b) $a = -0.8$ mm.

4 CONCLUSIONS

This paper deals with the use of a multistable compliant tensegrity structure for the application in a crawling motion system. Most of the known crawling motion system allow only a one-way motion or requires advanced demands to the operating actuator in order to realize a bidirectional uniaxial motion. In this paper a crawling motion system basing on a multistable tensegrity structure is modeled. The tensegrity structure enables multiple stable equilibrium configurations and is in contact to horizontal plane due to gravity. As consequence of the acting gravitational forces the application of certain equilibrium states initiates a tilting sequence. Hence, the mode of the entire motion system is changing. Moreover, total different dynamical properties result for the identical actuation of the system. Transient simulations are evaluated for selected parameter values of the tensegrity structure and the steady state solution which assumed after 1000 actuation periods is considered. The motion behavior which is characterized by the steady state velocity is analyzed for the different equilibrium configurations as initial state and diverse friction properties. The results confirm that a feasible control of the direction of motion occurs utilizing the given multistability of the tensegrity structure. At total, these investigations show that, indeed, a bidirectional uniaxial motion can be realized by the use of only one actuator with a selected excitation frequency.

However, for a significant parameter range a change into an additional equilibrium state occurs. Because of the corresponding low potential energy, a reverse change into another equilibrium state seems to be difficult. Hence, after the occurrence of this critical state the motion system cannot be used anymore. Therefore, a prototype should be equipped with safeguards like mechanical stops which prohibt a change into that critical equilibrium state.

Moreover, the authors target the development of a prototype as well as the experimental validation of the theoretical results shown in this paper.

ACKNOWLEDGEMENTS

This work is supported by the Deutsche Forschungsgemeinschaft (DFG project BO4114/2-1).

REFERENCES

Böhm, V., Sumi, S., Kaufhold, T., et al. (2017). Compliant multistable tensegrity structures. *Mechanism and Machine Theory*, 115:130 – 148.

Böhm, V., Zeidis, I., and Zimmermann, K. (2013). Dynamic analysis of a simple planar tensegrity structure for the use in vibration driven locomotion systems. In *12th Conference on Dynamical Systems - Theory and Applications*, pages 341–352.

Böhm, V., Zeidis, I., and Zimmermann, K. (2015). An approach to the dynamics and control of a planar tensegrity structure with application in locomotion systems. *International Journal of Dynamics and Control*, 3(1):41–49.

Böhm, V. and Zimmermann, K. (2013). Vibration-driven mobile robots based on single actuated tensegrity structures. In *2013 IEEE International Conference on Robotics and Automation*, pages 5475–5480.

Bolotnik, N., Zeidis, I., Zimmermann, K., et al. (2006). Dynamics of controlled motion of vibration-driven systems. *Journal of Computer and Systems Sciences International*, 45(5):831–840.

Chen, L. H., Kim, K., Tang, E., et al. (2017). Soft spherical tensegrity robot design using rod-centered actuation and control. *Journal of Mechanisms and Robotics*, 9(2):025001–025001–9.

Fang, H.-B. and Xu, J. (2011). Dynamic analysis and optimization of a three-phase control mode of a mobile system with an internal mass. *Journal of Vibration and Control*, 17(1):19–26.

Fang, H.-B. and Xu, J. (2012). Controlled motion of a two-module vibration-driven system induced by internal acceleration-controlled masses. *Archive of Applied Mechanics*, 82(4):461–47.

Hustig-Schultz, D., SunSpiral, V., and Teodorescu, M. (2016). Morphological design for controlled tensegrity quadruped locomotion. In *2016 IEEE/RSJ International Conference on Intelligent Robots and Systems (IROS)*, pages 4714–4719.

Khazanov, M., Jocque, J., and Rieffel, J. (2014). Evolution of locomotion on a physical tensegrity robot. *14th International Conference on the Synthesis and Simulation of Living Systems*, pages 232–238.

Kim, K., Chen, L. H., Cera, B., et al. (2016). Hopping and rolling locomotion with spherical tensegrity robots. In *2016 IEEE/RSJ International Conference on Intelligent Robots and Systems (IROS)*, pages 4369–4376.

Liu, H., Yu, Y., Sun, P., et al. (2016). Motion analysis of the four-bar tensegrity robot. In *2016 IEEE International Conference on Mechatronics and Automation*, pages 1483–1488.

Rieffel, J. A., Valer-Cuevas, F. J., and Lipson, H. (2010). Morphological communication: exploiting coupled dynamics in a complex mechanical structure to achieve locomotion. *Journal of the Royal Society Interface*, 7(45):613–621.

Sabelhaus, A. P., Bruce, J., Caluwaerts, K., et al. (2015). System design and locomotion of superball, an untethered tensegrity robot. In *2015 IEEE International Conference on Robotics and Automation (ICRA)*, pages 2867–2873.

Schorr, P., Sumi, S., Böhm, V., et al. (2017). Dynamical investigation of a vibration driven locomotion system

based on a multistable tensegrity structure. In *14th Conference on Dynamical Systems - Theory and Applications*, pages 485–496.

Steigenberger, J. and Behn, C. (2012). *Worm-Like Locomotion Systems. An intermediate theoretical Approach*. De Gruyter Oldenbourg.

Sumi, S., Böhm, V., and Zimmermann, K. (2017). A multistable tensegrity structure with a gripper application. *Mechanism and Machine Theory*, 114:204 – 217.

Tietz, B. R., Carnahan, R. W., Bachmann, R. J., et al. (2013). Tetraspine: Robust terrain handling on a tensegrity robot using central pattern generators. In *2013 IEEE/ASME International Conference on Advanced Intelligent Mechatronics*, pages 261–267.

Zimmermann, K., Zeidis, I., and Behn, C. (2009a). *Mechanics of Terrestrial Locomotion with a Focus on Nonpedal Motion Systems*. Springer.

Zimmermann, K., Zeidis, I., Bolotnik, N., et al. (2009b). Dynamics of a two-module vibration-driven system moving along a rough horizontal plane. *Multibody System Dynamics*, 22(2):199–219.

Zimmermann, K., Zeidis, I., and Pivovarov, M. (2013). Dynamics of two interconnected mass points in a resistive medium. *Differential Equations and Dynamical Systems*, 21(1):21–28.

SCITEPRESS
SCIENCE AND TECHNOLOGY PUBLICATIONS